Nuclear Inst. and Methods in Physics Research, A 886 (2018) 24–29

Contents lists available at ScienceDirect

Nuclear Inst. and Methods in Physics Research, A

journal homepage: www.elsevier.com/locate/nima

Live event reconstruction in an optically read out GEM-based TPC

F.M. Brunbauer [a,b,*], G. Galgóczi [a], D. Gonzalez Diaz [a,c], E. Oliveri [a], F. Resnati [a], L. Ropelewski [a], C. Streli [b], P. Thuiner [a], M. van Stenis [a]

[a] CERN, 385 Route de Meyrin, 1217 Meyrin, Geneva, Switzerland
[b] Technische Universität Wien, Karlsplatz 13, 1040 Wien, Austria
[c] Uludağ University, Özlüce Mahallesi, 16059 Bursa, Turkey

ARTICLE INFO

Keywords:
GEM detectors
Micro pattern gas chambers
Optical readout
Scintillation
Reconstruction
Time projection chambers

ABSTRACT

Combining strong signal amplification made possible by Gaseous Electron Multipliers (GEMs) with the high spatial resolution provided by optical readout, highly performing radiation detectors can be realized. An optically read out GEM-based Time Projection Chamber (TPC) is presented. The device permits 3D track reconstruction by combining the 2D projections obtained with a CCD camera with timing information from a photomultiplier tube. Owing to the intuitive 2D representation of the tracks in the images and to automated control, data acquisition and event reconstruction algorithms, the optically read out TPC permits live display of reconstructed tracks in three dimensions. An Ar/CF_4 (80/20%) gas mixture was used to maximize scintillation yield in the visible wavelength region matching the quantum efficiency of the camera. The device is integrated in a UHV-grade vessel allowing for precise control of the gas composition and purity. Long term studies in sealed mode operation revealed a minor decrease in the scintillation light intensity.

1. Introduction

The universality of Time Projection Chambers (TPCs) [1] makes them an attractive detector concept for a wide range of applications. To permit an accurate 3D reconstruction of particle tracks, the 2D projection on the endcap of a TPC must be recorded with possibly high spatial resolution. Additionally, the drift time information used to calculate the Z-coordinate of a particle track must be obtained with possibly high time resolution.

To enable the detection of various types of radiation from low-energy X-rays to highly ionizing alpha particles, robust signal amplification technologies such as Gaseous Electron Multipliers (GEMs) can be employed [2]. This variety of MicroPattern Gaseous Detectors (MPGDs) is composed of thin perforated foils with a conductor–insulator–conductor structure and allows for high electron multiplication factors by avalanche amplification in high electric field regions in the GEM holes with typical diameters of tens of micrometers. Employing multiple GEMs as consecutive amplification stages allows high effective charge gain factors [3] while still operating the detector in a stable regime. MPGD amplification stages such as triple-GEMs are therefore a high potential technology for TPC endcaps [4] providing high signal amplification and detection of weakly ionizing particles in the active volume. MPGDs are at the core of multiple ongoing detector upgrades and developments. The TPC of the ALICE experiment is currently undergoing an upgrade to employ a GEM-based readout [5], while the ATLAS collaboration is developing a muon spectrometer readout based on Micromegas, which can sustain high particle fluxes and is capable of achieving high spatial resolution [6]. In view of directional dark matter search experiments, optically read out GEM-based TPCs have been suggested and investigated as a candidate technology for providing accurate information about electron and nuclear recoil tracks [7].

Aiming at high spatial resolution in the readout of the endcaps of a TPC, optical readout is an attractive alternative to commonly used electronic readout concepts. Optical readout is based on the recording of scintillation light emitted in the gas in the active volume and has previously been shown to allow for high spatial resolution [8]. The optical readout concept provides a good track recognition capability as already demonstrated in imaging chambers based on parallel-grid chambers [9]. Coupling MPGDs such as GEMs with optical readout allows for high signal amplification as well as good position resolution and comes with the additional advantage of high signal-to-noise ratios and the inherent insensitivity to electric noise.

Optically read out TPCs employing combined readout with cameras and Photomultiplier Tubes (PMTs) have previously been developed

* Corresponding author at: CERN, 385 Route de Meyrin, 1217 Meyrin, Geneva, Switzerland.
E-mail address: florian.brunbauer@cern.ch (F.M. Brunbauer).

https://doi.org/10.1016/j.nima.2017.12.077
Received 10 August 2017; Received in revised form 23 December 2017; Accepted 27 December 2017
Available online 29 December 2017

for the study of rare decay modes and proton spectroscopy [10–12]. Using multistep avalanche chambers or GEMs as amplification and scintillation stages and operating in Ar–He gas mixtures with small additives of triethylamine or N_2, these previous works successfully demonstrated the applicability of optical TPCs for imaging of two-proton decays of ^{45}Fe nuclei [12] or proton spectroscopy of ^{48}Ni, ^{46}Fe and ^{44}Cr [11]. A similar readout concept has also been implemented by the DMTPC project, which aims at observing dark matter interactions by determining the energy and direction of nuclear recoils [13]. Optically read out TPCs have also been used in nuclear astrophysics experiments such as studies with gamma-ray beams [14,15].

We present a TPC based on a triple-GEM amplification stage optically read out by a high-resolution CCD camera, which provides an image of the 2D projection of alpha tracks, and a PMT, which simultaneously provides timing information to perform 3D track reconstruction. Using an Ar/CF_4 gas mixture with scintillation light emission in the visible wavelength regime, emitted light can be recorded without the need for wavelength shifters. The operation of the presented device is fully automated and allows for live 3D reconstruction and display of alpha particle tracks. Additionally, the described detector is built to highest purity requirements and demonstrates the possibility to realize a sealed TPC based on optically read out MPGDs.

2. Experimental methods

The drift volume of the presented optically read out GEM-based TPC is formed by a circular field shaper with a length of 10 cm and a diameter of 10 cm, which is coupled to a triple-GEM with an active region of 10×10 cm^2. These two elements are placed in a UHV-grade vessel to allow for a highly controlled environment and a pure gas filling. All components of the detector vessel are sealed by Cu gaskets. Inside the gas volume, the usage of low-outgassing materials such as oxygen-free Cu for the field shaper electrodes, ceramic for the GEM frames and polyether ether ketone (PEEK) for a holder for the triple-GEM stack ensures high gas purity and permits the operation of the TPC in flushed as well as sealed modes. Electrical connections are made by clamping to avoid the use of solder in the gas volume and all-metal valves and pressure transducers were used. Two borosilicate viewports 63 mm in diameter on opposite sides of the vessel allow the optical readout of scintillation light in the visible wavelength regime produced in the gas volume. Behind these viewports, a CCD camera (QImaging Retiga R6) facing the last GEM of the triple-GEM stack and a PMT (Hamamatsu R375) facing the cathode mesh used to define the drift field are placed as shown in Fig. 1.

The 6-megapixel CCD camera with bulb-mode triggering capabilities features a 12.5×10 mm^2 imaging sensor with pixels of 4.54×4.54 μm^2. The imaging sensor is cooled to −20 °C to achieve a low read noise of 5.7 electrons (RMS) and a dark current rate of 0.00017 electrons/pixel/second. Imaging the full active area of the detector, a magnification factor of approximately 10 results in an effective pixel size of about 45×45 μm^2 on the imaging plane. The PMT was operated at a gain of approximately 2×10^6 in order to be sensitive to primary scintillation signals.

The employed GEM foils feature holes with a diameter of 70 μm and a hole pitch of 140 μm, which are chemically etched into the Cu-polyimide-Cu composite material by a double-mask etching technique. For highly ionizing alpha particles, the triple-GEM was operated at moderate gains of several 10^3. A stainless steel mesh-cathode is used together with the field shaper composed of multiple ring-shaped Cu electrodes connected with high-voltage resistors to define the electric drift field in the active volume of the TPC. The presented setup permits drift fields of up to 500 V/cm and can also be used with significantly lower drift fields of tens of V/cm due to the low level of outgassing and the resulting high gas quality in the detector vessel minimizing the significance of attachment and loss of primary electrons.

The PMT facing the cathode is used to record both the primary scintillation signal as well as the secondary scintillation light emitted after primary electrons have drifted towards and reached the triple-GEM and have been amplified in the high electric field regions inside the GEM holes. Due to the optical transparency of the GEM foils of about 20%, the PMT may record scintillation light emitted from all three GEMs in the multiplication stage with the majority of the detected photons originating from the third GEM. The acceptance factor for the detection of secondary scintillation photons by the PMT was determined to be approximately 6.4×10^{-4} by ray tracing simulations and by taking into account the emission spectrum of the Ar/CF_4 gas mixture, the wavelength-dependent transmission of the borosilicate viewport and the quantum efficiency of the PMT.

As signal amplification in the GEM stack happens fast due to high electric fields inside the GEM holes and transfer fields of about 2 kV/cm between GEM foils, this impacts the timing characteristics of the signals observed by the PMT only minimally. The CCD camera facing the bottom of the triple-GEM records integrated images of the 2D projection of the particle track on the GEM stack, which acts as the endcap of the TPC. Due to state-of-the-art imaging sensors not being sensitive to a level where single photon detection is feasible and the low optical transparency of the triple-GEM stack, the CCD camera is not capable of recording primary scintillation signals and only records the much stronger secondary scintillation light emitted during avalanche amplification in the GEM holes.

To maximize the signal-to-noise ratio both in the images recorded with the CCD as well as in the PMT response, an Ar/CF_4 gas mixture with a composition of 80/20% (by volume) was used. The maximum achieved light yield with this mixture was 0.3 photons per secondary electron produced during electron avalanche multiplication. The emission spectrum of the scintillation light of this mixture features a pronounced intensity peak at 630 nm in the visible wavelength regime. Therefore, it can be efficiently recorded by the CCD camera, which has a quantum efficiency peaking at 75% for 600 nm. The quantum efficiency of the CCD and the PMT at 630 nm were 73% and 11%, respectively. This match between the scintillation light emission spectrum and the wavelength-dependent quantum efficiency of the CCD permits high light sensitivity.

Before the initial gas filling, the detector vessel is pumped to a pressure of about 10^{-6} mbar with a turbomolecular pump. Extended pumping for 48 h is used to minimize the residual outgassing from the detector elements inside the chamber. Subsequently, the detector vessel is sealed off with an all-metal valve. Only after extensive purging of all gas lines is the detector filled with the desired gas mixture to a pressure of 1 bar.

To permit live 3D reconstruction of alpha particle tracks in the TPC, a triggering, data acquisition and reconstruction algorithm was developed and implemented both in hardware as well as software. PMT signals are recorded by a digital storage oscilloscope (DSO) (LeCroy WaveRunner 625Zi, 2.5 GHz, 40 GS/s) and the intense and unambiguous secondary scintillation signals are used as a trigger to identify the occurrence of a new event. These trigger signals are used to stop the exposure of the CCD camera as well as to trigger the data acquisition of the PMT waveform from the DSO and the recorded image from the CCD camera via a microcontroller coupled to a control script executed on a standard desktop computer. Once a PMT waveform and the matching CCD image have been transferred to the computer, a reconstruction algorithm automatically performs a 3D reconstruction of the particle track, stores the data for later offline analysis and displays a 3D representation of the event on-screen.

The exposure time of the recorded CCD images depends on the time between subsequent events and varies from image to image due to the employed bulb mode triggering. Therefore, the noise level due to the dark current of the pixels of the CCD camera, which depends on the exposure time, is different for each image. For the used imaging sensor, the read noise of 5.7 electrons (RMS) is much more significant than the dark current rate of 0.00017 electrons/pixel/second for typical exposure times of less than 1 s.

Alpha particles originating from the decay of ^{220}Rn were used for the demonstration of the track reconstruction capabilities of the presented

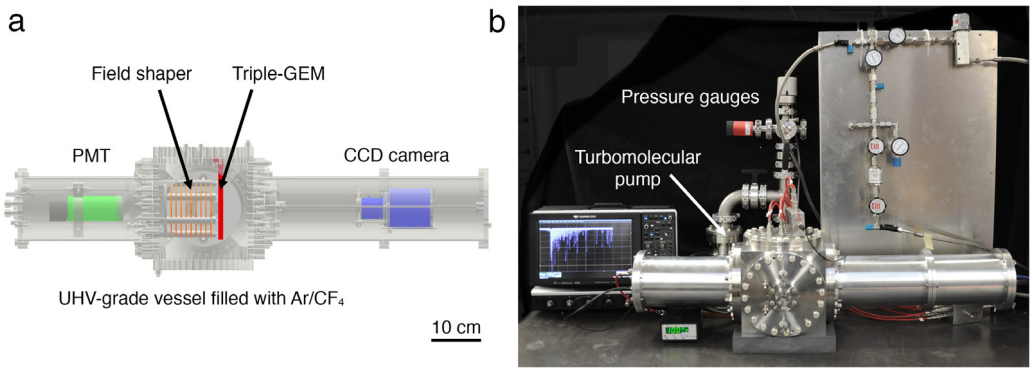

Fig. 1. (a) Schematic of GEM-based TPC read out by PMT and CCD camera. The 10 cm diameter field shaper and the triple-GEM with an active area of 10×10 cm^2 are placed inside of a UHV-grade vessel while the readout elements are placed behind borosilicate viewports. (b) Setup with optically read out TPC, oscilloscope for PMT readout, turbomolecular pump and pressure gauges for cleaning the chamber for high-purity operation.

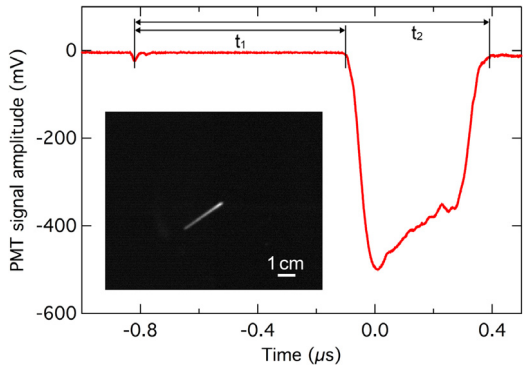

Fig. 2. Typical PMT waveform exhibiting primary and secondary scintillation pulses of an alpha particle in the TPC. The times t_1 and t_2 between the primary scintillation and the leading and trailing edges of the secondary scintillation pulse are used to determine the Z-coordinates of the particle track. Inset: CCD image of alpha track with signal-to-noise ratio of 48 and visible Bragg peak.

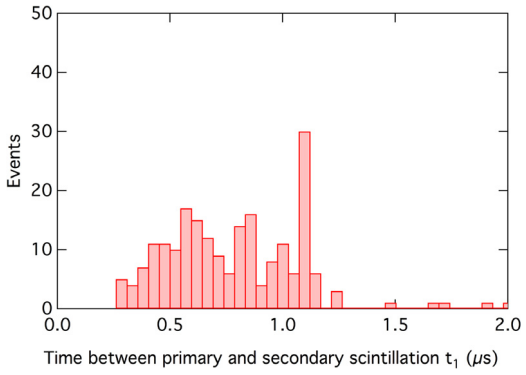

Fig. 3. Distribution of times t_1 between primary scintillation and leading edge of secondary scintillation. Electron drift times for alpha particles originating along the length of the active conversion volume are reflected in the distribution. A pronounced peak around 1.1 μs corresponding to electrons drifting along the entire length of the drift volume of 10 cm is attributed to the accumulation of decaying nuclei on the cathode.

device. A ^{228}Th source was used to flush ^{220}Rn into the detector vessel where decays of ^{220}Rn resulted in 6.4 MeV alpha particles with a random distribution of orientations and spatial origins. A number of alpha particles were therefore not contained in the active drift volume of the TPC. In the presented case of alpha particles from the decay of ^{220}Rn, partially contained events can be easily identified by the length of their tracks or by their deposited energy and could therefore easily be excluded from further analysis. More generally, tracks crossing the borders of the active region could be identified and excluded as partially contained events.

3. Results and discussion

An optically read out GEM-based detector was operated as a TPC to demonstrate the live event reconstruction capabilities of the presented device for alpha particles. An exemplary PMT waveform is shown in Fig. 2 together with a CCD image of an alpha track.

Events without matching PMT waveforms and images are discarded from further analysis, which may include exposures showing more than a single alpha track or waveforms without an identifiable primary scintillation signal. About two thirds of events did not show identifiable primary scintillation signals, which is mainly attributed to limited geometric acceptance and partially contained events, and more than 90% of images showed only a single alpha track. For accepted events with matching PMT waveforms and CCD images and identifiable primary scintillation signals, the times t_1 and t_2 as shown in Fig. 2 between the primary scintillation pulse and the leading and trailing edges of the secondary scintillation pulse are extracted. The distribution of drift times t_1 between the primary scintillation and the leading edge of the secondary scintillation pulse is shown in Fig. 3.

Multiplying the shorter time t_1 between the primary scintillation pulse and the beginning of the secondary one by the determined electron drift velocity in the drift region yields the Z-coordinate of the track point closest to the GEMs. Equivalently, multiplying the longer time t_2 by the electron drift velocity provides the Z-coordinate of the track point closest to the cathode. This method introduces some uncertainty in the angle of tracks almost perpendicular or parallel to the GEMs. For parallel tracks, the width of the secondary scintillation pulse is very short, which negatively impacts the determination of Z-coordinates from the difference in electron drift times. For perpendicular tracks, the 2D projection of the track is very short and it may not be possible to determine the orientation of the track from the position of the Bragg peak in the CCD image.

The angular resolution of the presented device could not be determined as the geometry of the high purity vessel did not allow a selection of incident particle angles and relied on a gaseous source with random decay origins and orientations. Exemplary schematic representations of two extreme cases of track angles are shown in Fig. 4.

Subsequently, the alpha track is extracted from the CCD image by employing a flood-fill algorithm applied to a binary image obtained from the original grayscale image by a threshold of 5 standard deviations above the background level. The background level and the standard deviation of the background intensity are extracted for each image individually. The flood-fill algorithm identifies all bright pixels in the

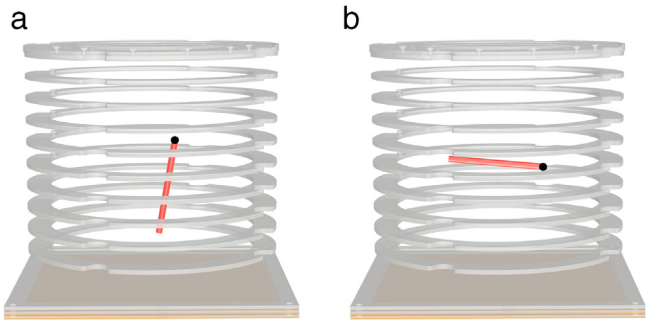

Fig. 4. Reconstructed alpha tracks visualized inside the field cage with GEMs at the bottom with black dots indicating origins of tracks. (a) Long secondary scintillation pulses characterize tracks nearly perpendicular to the GEMs. (b) Short secondary scintillation pulses correspond to nearly parallel tracks.

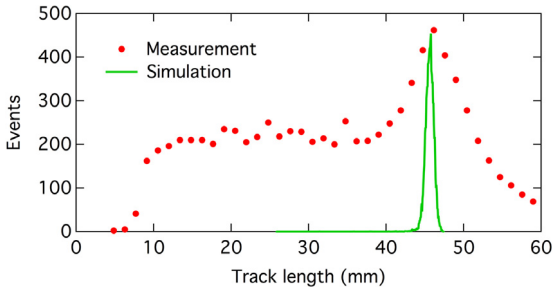

Fig. 5. The peak of the distribution of reconstructed alpha track lengths representing fully contained tracks agrees with a comparative simulation. Shorter track lengths correspond to partially contained alpha tracks.

binary image connected to a start pixel on the track. This algorithm excludes individual hot pixels in the recorded images and is thus suited to identify dominant tracks and their extent in the images.

The X-Y-projection resulting from this analysis is then combined with the Z-coordinates obtained from the drift times of the closest and farthest track points to arrive at a 3D representation of the straight alpha track. By comparing energy loss profiles from PMT waveforms of secondary scintillation signals and from line profiles of the pixel value intensity along tracks in the CCD images, the orientation of tracks can be determined. The unambiguous presence of Bragg peaks in CCD images as well as in PMT waveforms, as shown in Fig. 2, allows for an orientation of tracks and permits the identification of the start and end points of alpha tracks.

The drift velocity in the employed gas mixture for different electric fields was determined from the distribution of drift times and the length of the field shaper. The drift times of a number of alpha particles from a gaseous source in the field shaper were measured. The known length of the field shaper was subsequently divided by the longest observed drift time to obtain the drift velocity. For a drift field of 400 V/cm in the used Ar/CF_4 (80/20%) mixture, a drift velocity of 8.2 cm/μs was obtained. This value is slightly lower than the drift velocity of 10.2 cm/μs in an Ar/CF_4 (90/10%) mixture measured by P. Colas et al. [16], which may be explained by the larger fraction of CF_4 in the presented case. The conversion factor from pixels in the CCD image to spatial X-Y coordinates was determined by counting GEM holes in a line profile of the pixel value intensity in a CCD image and dividing the length of the line profile in pixels by the distance obtained from the number of holes and the known pitch of 140 μm between individual holes.

The automated triggering, data acquisition and 3D reconstruction algorithm, which was developed and employed to combine the information from the CCD camera and the PMT into a live display of alpha particle events in the TPC, enables the recording and reconstruction of events at a rate of approximately 2 Hz. Since the used ^{220}Rn source achieved a low rate of alpha decays, this was sufficient to record a reasonable fraction of the events. In the presented setup, the rate-limiting factor was the communication between the data acquisition devices and the desktop computer running the control and reconstruction algorithms.

The finite active drift volume of the TPC results in a number of alpha particles not being fully contained. At atmospheric pressure, the distribution of reconstructed alpha track lengths shown in Fig. 5 was observed.

The peak between 45 and 50 mm corresponds to alpha tracks fully contained in the drift volume while shorter recorded track lengths result from partially contained events. The broadening of the peak may be due to inaccuracies in the determination of the track length for tracks nearly parallel or perpendicular to the GEMs. While the high spatial resolution of the CCD images provides good measurements of the lengths of the 2D projections of tracks, inaccuracies in the determination of electron drift times from PMT waveforms might contribute to the widened track length distribution. For some particle tracks that are almost parallel to the GEMs, the reconstruction algorithm could not accurately determine the small time differences between primary and secondary scintillation pulses, which resulted in errors in the reconstructed track lengths. For tracks almost perpendicular to the GEMs, the Z-projections are large and even small inaccuracies in the determination of the time differences between primary and secondary scintillation pulses might significantly influence the determined track lengths. A comparative Geant4 simulation of the ionization of an Ar/CF_4 (80/20%) mixture by 6.4 MeV alpha particles yielded a track length distribution in agreement with the peak of the experimentally observed distribution.

The trend of the secondary scintillation light intensity for radiation events with a known constant energy was recorded over an extended period of time while the detector volume was sealed without gas recirculation to investigate the possibility of operating the detector in sealed mode. 5.9 keV ^{55}Fe X-rays were aimed into the active volume of the UHV-grade chamber through a thin metallic window in the position where otherwise the viewport for the PMT was located. The X-ray source was placed directly in front of the thin metallic window facing the cathode of the detector. The integral of the secondary scintillation light signal was computed from the acquired PMT waveforms. Energy spectra as shown in the inset in Fig. 6 were compiled from the acquired PMT signals. The energy spectra displayed both escape and full energy peaks of ^{55}Fe with an energy resolution of 32% FWHM at 5.9 keV. The trend of the scintillation light intensity was investigated by recording energy spectra in intervals of 60 min and plotting the position of the full energy peak over time. Operating the detector for almost six days in sealed mode, the scintillation light intensity decreased by approximately 5%. Fig. 6 shows the minor decrease in light intensity over time, which is attributed to a slight contamination of the gas in the chamber as a result of outgassing from the GEM foils and other materials used in the detector assembly. Nevertheless, the small signal loss over several days suggests that a sealed TPC based on the presented concept is feasible.

4. Conclusion

A TPC integrated in a high-purity vessel allowing for extended sealed mode operation is presented. Primary scintillation of alpha particles in the Ar/CF_4 gas mixture was recorded by a PMT. A triple-GEM multiplication stage was employed to amplify the primary electrons and achieve secondary scintillation light signals strong enough to be read out by a CCD camera. The 2D projection imaged by the camera was combined with depth information obtained from the time between primary and secondary scintillation signals recorded by the PMT to enable 3D event reconstruction of 6.4 MeV alpha tracks. A hardware-based triggering mechanism was combined with device control, data acquisition and event reconstruction algorithms to fully automate data taking and 3D track reconstruction. This permits live display of alpha tracks in the

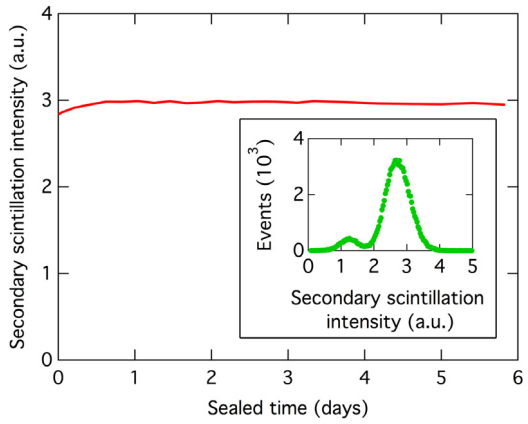

Fig. 6. The trend of the full energy peak position obtained from secondary scintillation light spectra over six days displays minor signal degradation. Inset: ^{55}Fe energy spectrum obtained from integration of secondary scintillation pulses from PMT featuring escape and full energy peaks.

active volume of the TPC. The length of fully contained alpha tracks was measured and shown to agree with a comparative simulation. Bragg peaks were clearly identified both in the secondary scintillation signals recorded by the PMT as well as in line profiles extracted from CCD images and permitted a determination of the orientation of the tracks.

The presented 3D event reconstruction from 2D images and depth information from the electron drift time between primary and secondary scintillation is only compatible with straight tracks such as alpha tracks and may yield ambiguous results for curved or more complex particle trajectories. However, the optically read out GEM-based TPC can readily be modified to enable 3D reconstruction of arbitrary particle tracks by combining optical and electronic signal readout. By placing a transparent multi-pad anode below the triple-GEM stack, electronic signals and signal arrival times can be recorded with fast readout electronics while allowing scintillation light to pass through the anode to be read out with a camera. Transparent anodes can be manufactured from indium tin oxide (ITO) and structured by optical lithography and etching procedures. The presented optically read out TPC has been equipped with transparent ITO-based anodes with either 5×5 pads or 48 strips and electronic signals containing electron arrival time information have successfully been acquired while simultaneously recording scintillation light with a camera placed behind the anode. This combination of optical and electronic readout potentially permits 3D reconstruction of complex particle trajectories by combining the high spatial resolution of optical readout with the fast readout of electronic signals. In this case, the reduced requirements in the granularity of the electronic readout require a lower number of channels to be read out, while spatial information is provided by the optical readout with high position resolution and without the need for extensive image reconstruction algorithms. The developed triggering and data acquisition algorithm for live event reconstruction could also be used for minimum ionizing particles and low-energy recoil events recorded with a combination of optical and electronic readout. Depending on the camera technology used for optical readout, GEM gains of several 10^3 to 10^4 would result in strong enough secondary scintillation light signals to record images with acceptable signal-to-noise ratios.

The discussed device demonstrates the advantages of the optical readout of MPGDs for applications such as track reconstruction in TPCs. The spatial resolution permitted by high resolution cameras combined with the intuitive event reconstruction permitted by optical 2D images and PMT waveforms makes this technology an attractive approach for particle detectors. Optically read out GEM-based TPCs present a high potential candidate for nuclear physics experiments studying rare events such as nuclear recoils associated with weakly ionizing particles and nuclear astrophysics experiments. Moreover, the shown possibility to operate the device in sealed mode for extended periods of time introduces the possibility to realize portable TPC-like detectors relying on MPGDs for signal amplification and optical readout for effective data acquisition. With an integrated calibration mechanism or by using getters to extend the achievable time in sealed mode operation with acceptable decrease in signal intensity, versatile portable devices may be feasible. The high dynamic range and the good spatial resolution of optically read out GEM-based TPCs make them well suited for providing topology information for a variety of events.

Acknowledgment

The authors gratefully acknowledge support in designing the presented device by Christophe Bault (CERN, Geneva, Switzerland).

References

[1] D.R. Nygren, The time projection chamber - A new 4pi detector for charged particles, EConf. C740805 (1974) 58–78.
[2] F. Sauli, GEM: A new concept for electron amplification in gas detectors, Nucl. Instruments Methods Phys. Res. Sect. A: Accel. Spectrometers, Detect. Assoc. Equip. 386 (1997) 531–534. http://dx.doi.org/10.1016/S0168-9002(96)01172-2.
[3] B. Ketzer, M.C. Altunbas, K. Dehmelt, J. Ehlers, J. Friedrich, B. Grube, S. Kappler, I. Konorov, S. Paul, A. Placci, L. Ropelewski, F. Sauli, L. Schmitt, F. Simon, Triple GEM tracking detectors for COMPASS, IEEE Trans. Nucl. Sci. 49 (II) (2002) 2403–2410. http://dx.doi.org/10.1109/TNS.2002.803891.
[4] S. Kappler, J. Kaminski, B. Ledermann, T. Müller, L. Ropelewski, F. Sauli, Design and construction of a GEM-TPC prototype for research and development purposes, IEEE Trans. Nucl. Sci. 51 (2004) 1524–1528. http://dx.doi.org/10.1109/TNS.2004.832897.
[5] J. Alme, Y. Andres, H. Appelshuser, S. Bablok, N. Bialas, R. Bolgen, U. Bonnes, R. Bramm, P. Braun-Munzinger, R. Campagnolo, P. Christiansen, A. Dobrin, C. Engster, D. Fehlker, Y. Foka, U. Frankenfeld, J.J. Gaardhøje, C. Garabatos, P. Glssel, C. Gonzalez Gutierrez, P. Gros, H.A. Gustafsson, H. Helstrup, M. Hoch, M. Ivanov, R. Janik, A. Junique, A. Kalweit, R. Keidel, S. Kniege, M. Kowalski, D.T. Larsen, Y. Lesenechal, P. Lenoir, N. Lindegaard, C. Lippmann, M. Mager, M. Mast, A. Matyja, M. Munkejord, L. Musa, B.S. Nielsen, V. Nikolic, H. Oeschler, E.K. Olsen, A. Oskarsson, L. Osterman, M. Pikna, A. Rehman, G. Renault, R. Renfordt, S. Rossegger, D. Rhrich, K. Røed, M. Richter, G. Rueshmann, A. Rybicki, H. Sann, H.R. Schmidt, M. Siska, B. Sitr, C. Soegaard, H.K. Soltveit, D. Soyk, J. Stachel, H. Stelzer, E. Stenlund, R. Stock, P. Strme, I. Szarka, K. Ullaland, D. Vranic, R. Veenhof, J. Westergaard, J. Wiechula, B. Windelband, The ALICE TPC, a large 3-dimensional tracking device with fast readout for ultra-high multiplicity events, Nucl. Instruments Methods Phys. Res. Sect. A: Accel. Spectrometers, Detect. Assoc. Equip. 622 (2010) 316–367. http://dx.doi.org/10.1016/j.nima.2010.04.042.
[6] M. Bianco, Micromegas detectors for the muon spectrometer upgrade of the ATLAS experiment, Nucl. Instruments Methods Phys. Res. Sect. A: Accel. Spectrometers, Detect. Assoc. Equip. 824 (2016) 496–500. http://dx.doi.org/10.1016/j.nima.2015.11.076.
[7] N.S. Phan, R.J. Lauer, E.R. Lee, D. Loomba, J.A.J. Matthews, E.H. Miller, GEM-based TPC with CCD imaging for directional dark matter detection, Astropart. Phys. 84 (2016) 82–96. http://dx.doi.org/10.1016/j.astropartphys.2016.08.006.
[8] F.A.F. Fraga, L.M.S. Margato, S.T.G. Fetal, M.M.F.R. Fraga, R. Ferreira Marques, A.J.P.L. Policarpo, Optical readout of GEMs, Nucl. Instruments Methods Phys. Res. Sect. A: Accel. Spectrometers, Detect. Assoc. Equip. 471 (2001) 125–130. http://dx.doi.org/10.1016/S0168-9002(01)00972-X.
[9] G. Charpak, J.P. Fabre, F. Sauli, M. Suzuki, W. Dominik, An optical, proportional, continuously operating avalanche chamber, Nucl. Inst. Methods Phys. Res. A 258 (1987) 177–184. http://dx.doi.org/10.1016/0168-9002(87)90054-4.
[10] P. Fonte, A. Breskin, G. Charpak, W. Dominik, F. Sauli, Beam test of an imaging high-density projection chamber, Nucl. Instruments Methods Phys. Res. Sect. A: Accel. Spectrometers, Detect. Assoc. Equip. 283 (1989) 658–664. http://dx.doi.org/10.1016/0168-9002(89)91436-8.
[11] M. Pomorski, M. Pfützner, W. Dominik, R. Grzywacz, A. Stolz, T. Baumann, J.S. Berryman, H. Czyrkowski, R. Dąbrowski, A. Fijałkowska, T. Ginter, J. Johnson, G. Kamiński, N. Larson, S.N. Liddick, M. Madurga, C. Mazzocchi, S. Mianowski, K. Miernik, D. Miller, S. Paulauskas, J. Pereira, K.P. Rykaczewski, S. Suchyta, Proton spectroscopy of 48Ni, 46Fe, and 44Cr, Phys. Rev. C. 90 (2014) 14311. http://dx.doi.org/10.1103/PhysRevC.90.014311.
[12] W. Dominik, Z. Janas, A. Korgul, K. Miernik, M. Pfützner, M. Sawicka, A. Wasilewski, Optical time projection chamber for imaging of two-proton decay of 45 Fe nucleus, IEEE Trans. Nucl. Sci. 52 (2005) 2895–2899.

[13] G. Sciolla, T.D. Collaboration, The DMTPC project, J. Phys. Conf. Ser. 179 (2009) 12009. http://dx.doi.org/10.1088/1742-6596/179/1/012009.

[14] M. Gai, M.W. Ahmed, S.C. Stave, W.R. Zimmerman, A. Breskin, B. Bromberger, R. Chechik, V. Dangendorf, T. Delbar, R.H. France, S.S. Henshaw, T.J. Kading, P.P. Martel, J.E.R. McDonald, P.-N. Seo, K. Tittelmeier, H.R. Weller, a H. Young, An optical readout TPC (O-TPC) for studies in nuclear astrophysics with gamma-ray beams at HIγS 1, J. Instrum. 5 (2010) 12004–P12004. http://dx.doi.org/10.1088/1748-0221/5/12/P12004.

[15] W.R. Zimmerman, M.W. Ahmed, B. Bromberger, S.C. Stave, A. Breskin, V. Dangendorf, T. Delbar, M. Gai, S.S. Henshaw, J.M. Mueller, C. Sun, K. Tittelmeier, H.R. Weller, Y.K. Wu, Unambiguous identification of the second 2+ state in C12 and the structure of the hoyle state, Phys. Rev. Lett. 110 (2013) 1–5. http://dx.doi.org/10.1103/PhysRevLett.110.152502.

[16] P. Colas, A. Delbart, J. Derre, I. Giomataris, F. Jeanneau, V. Lepeltier, I. Papadopoulos, P. Rebourgeard, Electron drift velocity measurements at high electric fields, NIM. 478 (2002) 215–219.